Neuroscience 169 (2010) 98–108

CHRONIC FLUOXETINE TREATMENT INDUCES STRUCTURAL PLASTICITY AND SELECTIVE CHANGES IN GLUTAMATE RECEPTOR SUBUNITS IN THE RAT CEREBRAL CORTEX

E. AMPUERO,[a] F. J. RUBIO,[a] R. FALCON,[a] M. SANDOVAL,[a] G. DIAZ-VELIZ,[b] R. E. GONZALEZ,[a] N. EARLE,[a] A. DAGNINO-SUBIABRE,[c] F. ABOITIZ,[d] F. ORREGO[a] AND U. WYNEKEN[a]*

[a]*Laboratorio de Neurociencias, Universidad de los Andes, Santiago, Chile*

[b]*Facultad de Medicina, Universidad de Chile, Santiago, Chile*

[c]*Laboratorio de Neurobiologia y Conducta, Facultad de Medicina, Universidad Catolica del Norte, Santiago, Chile*

[d]*Departamento de Psiquiatria, Pontificia Universidad Catolica de Chile, Santiago, Chile*

Abstract—It has been postulated that chronic administration of antidepressant drugs induces delayed structural and molecular adaptations at glutamatergic forebrain synapses that might underlie mood improvement. To gain further insight into these changes in the cerebral cortex, rats were treated with fluoxetine (flx) for 4 weeks. These animals showed decreased anxiety and learned helplessness. N-methyl-D-aspartate (NMDA) and α-amino-3-hydroxy-5-methylisoxazole-4-propionate (AMPA) receptor subunit levels (NR1, NR2A, NR2B, GluR1 and GluR2) were analysed in the forebrain by both western blot of homogenates and immunohistochemistry. Both methods demonstrated an upregulation of NR2A, GluR1 and GluR2 that was especially significant in the retrosplenial granular b cortex (RSGb). However, when analysing subunit content in postsynaptic densities and synaptic membranes, we found increases of NR2A and GluR2 but not GluR1. Instead, GluR1 was augmented in a microsomal fraction containing intracellular membranes. NR1 and GluR2 were co-immunoprecipitated from postsynaptic densities and synaptic membranes. In the immunoprecipitates, NR2A was increased while GluR1 was decreased supporting a change in receptor stoichiometry. The changes of subunit levels were associated with an upregulation of dendritic spine density and of large, mushroom-type spines. These molecular and structural adaptations might be involved in neuronal network stabilization following long-term flx treatment.

Key words: antidepressants, glutamate, ionotropic receptors, dendritic spines, cerebral cortex.

The selective serotonin reuptake inhibitor fluoxetine (flx) is one of the most commonly prescribed antidepressant drugs. The mechanisms underlying its antidepressant action, however, are still unclear. Although serotonin levels rise rapidly after acute administration, several weeks are required before therapeutic benefits are achieved. The delayed onset of antidepressant action suggests that plastic changes over protracted periods of time might be causally related to the therapeutic effect. Repetitive antidepressant administration promotes plastic changes such as neurogenesis, synaptogenesis, neurotrophin signalling, and changes in chromatin structure and gene expression (Castren et al., 2007; Krishnan and Nestler, 2008; McClung and Nestler, 2008).

Increasing evidence implicates glutamatergic circuitries in these plastic changes (Popoli et al., 2002; Bleakman et al., 2007; Gould et al., 2008; Sanacora et al., 2008; O'Leary et al., 2009). We found that 2 weeks of flx treatment induced brain-derived neurotrophic factor (BDNF) signalling at excitatory forebrain synapses (Wyneken et al., 2006). Glutamatergic synapses are situated on dendritic spines containing postsynaptic densities (PSDs), which allow glutamate receptors to anchor through interactions with scaffolding proteins. Spines and PSDs are plastic structures, and large spines are associated with more efficient synapses (Kopec and Malinow, 2006). The development of dendritic spines begins with the formation of filopodia. After establishing contact with pre-synaptic terminals, they mature into spines acquiring thin, then stubby, and finally mushroom morphologies. The latter represent the most mature and stable spines.

Ionotropic glutamate receptors include the alpha-amino-3-hydroxy-5-methyl-4-isoxazole propionic acid (AMPA-R) and N-methyl-D-aspartate (NMDA-R) types. NMDA-Rs are heterotetramers composed of NR1 and NR2 subunits that coassemble to form a functional channel. A single NR1 subunit exists in eight splice isoforms, and there are four distinct NR2 subunits (NR2A–D). AMPA-Rs are homo- or heterotetramers composed mainly of GluR1 and 2/3 subunits in the adult forebrain. NMDA-R and AMPA-R subunit composition is a major determinant of biophysical properties, association to protein complexes, downstream signalling, receptor trafficking and synaptic targeting (Al-Hallaq et al., 2007; Shepherd and Huganir, 2007). Glutamate receptor availability determines spine structure, and NMDA-Rs, especially those containing NR2A subunits, are present in large and stable spines (Alvarez et al., 2007; Kobayashi et al., 2007). Similarly, GluR2 subunits promote the formation and growth of large spines (Saglietti et al., 2007; Medvedev et al., 2008; Chen et al., 2009).

*Corresponding author. Tel: +56-2-4129353; fax: +56-2-2141752.
E-mail address: uwyneken@uandes.cl (U. Wyneken).
Abbreviations: BDNF, brain-derived neurotrophic factor; EPM, elevated plus maze; flx, fluoxetine; FST, forced swim test; IHC, immunohistochemistry; NMDA, N-methyl-D-aspartate; NSF, novelty-suppressed feeding; PrL, prelimbic cortex; PSDs, postsynaptic densities; RSGb, retrosplenial granular b cortex; TST, tail suspension test; WB, western blots.

0306-4522/10 $ - see front matter © 2010 IBRO. Published by Elsevier Ltd. All rights reserved.
doi:10.1016/j.neuroscience.2010.04.035

The present study examined glutamate receptor levels following long-term flx treatment in the prelimbic (PrL), retrosplenial granular b (RSGb) and secondary motor (M2) cortices, as well as in subcellular fractions obtained from the forebrain. Spine morphology was analysed in the same regions. Our results strongly suggest that flx induces plastic changes in extensive forebrain networks that are consistent with a functional stabilization of synaptic connections.

EXPERIMENTAL PROCEDURES

Animals

We used adult male Sprague–Dawley rats (250–400 g) in all of the experiments. Procedures involving animals and their care were performed in accordance with the Universidad de los, Andes Bioethical Committee and the Guide for the Care and Use of Laboratory Animals from the National Institutes of Health. All efforts were made to minimize animal suffering. Flx at doses of 0.7 or 3.5 mg/kg (Ely-Lilly Co., Indianapolis, USA) or 0.9% NaCl (sal) were administered daily by i.p. injection between 9:00 and 10:00 AM for 28 days. Body weight was controlled daily and the percentage of weight gain was calculated. In total, 224 rats were sacrificed 24 h following the last flx or sal injection to perform immunohistochemistry (n=6 per group), Golgi staining (n=6 per group) or subcellular fractionation (n=10 per group, in total 10 independent preparations were performed). For immunohistochemistry or for Golgi staining, rats were sacrificed under ketamine (50 mg/kg) and xylazine (5 mg/kg) anaesthesia and then perfused intracardially with sal followed by 300 ml of 4% paraformaldehyde in PBS. After perfusion, brains were removed immediately and processed for immunohistochemistry or for Golgi staining.

Materials

All chemical reagents were purchased from Sigma (St Louis, MO, USA), unless otherwise stated. Protein G Sepharose was from Amersham Biosciences (Freiburg, Germany).

The primary antibodies used for immunohistochemistry (IHC), synaptic membrane staining and western blots (WB) were as follows: guinea pig anti-ProSAP2/Shank3 (synaptic membranes, 1:2000) (kindly donated by Eckart D. Gundelfinger at the Leibniz Institute for Neurobiology, Magdeburg, Germany); anti-GluR1 (synaptic membranes, 1:10; IHC, 1:50; WB, 1:1000), anti-GluR2 (synaptic membranes, 1:50; IHC, 1:400) and anti-NR2A (IHC, 1:100; Chemicon International, Temecula, CA, USA); anti-GluR2 (WB, 1:1000; BD Biosciences, Pharmingen, San Jose, CA, USA); anti-NR2A (synaptic membranes, 1:2000; WB, 1:1000; Millipore Corporation, MA, USA); anti-NR1 (IHC, 1:250; Pharmingen, San Diego, CA, USA); and anti-NR2B (IHC, 1:100; WB, 1:1000), anti-SAP102 (WB, 1:1000) and anti-PSD-95 (WB, 1:250; BD Transduction Laboratories, San Jose, CA, USA).

Behavioural studies

Rats were housed in groups of three in a 12-h (8:00–20:00) light/dark cycle at 22±1 °C with standard rodent pellet food and water available *ad libitum*. Each animal behaviour was evaluated only once, 24 h after the final injection using the following sequence: novelty-suppressed feeding (NSF), spontaneous motor activity, elevated plus maze (EPM), tail suspension test (TST) and the pretest session of the forced swim test (FST). The test session of the FST was applied on the second day (i.e., 48 h after the last drug injection). Scores were generated from live observations by an experimenter blinded to the treatment condition, and video sequences were used for later reanalysis when necessary.

Novelty-suppressed feeding test. The testing apparatus consisted of a plastic cage (80×70×40 cm^3) with its floor covered with 2 cm of wooden bedding. Twenty-four hours before behavioural testing (immediately following the last drug injection), animals were deprived of food in the home cage. At the time of testing, one food pellet was placed on a piece of round filter paper (10 cm in diameter) positioned in the centre of the box. The animal was placed in a corner of the cage. The latency to begin feeding was recorded (maximum time, 15 min). Afterwards, the amount of food consumed in 5 min in the home cage was measured.

Spontaneous motor activity. Rats were individually placed in a plexiglass cage (30×30×35 cm^3) located inside a soundproof chamber. The spontaneous motor activity and rearing was monitored during a period of 30 min and evaluated as described previously (Diaz-Veliz et al., 2004).

Elevated plus-maze. The apparatus consisted of a central platform (10×10 cm^2), two opposed open arms (50×10 cm^2) and two opposed closed arms of the same size with 40-cm-high opaque walls. The maze was elevated 83 cm above the ground. Each animal was placed at the centre of the maze facing one of the open arms. During a 5-min interval, the number of open and closed arms entries, plus the time spent in the open and closed arms were measured in dim light.

Tail suspension test. Rats were individually suspended by the tail to a horizontal ring stand bar (distance from the table, 40 cm) at 4–5 cm from the beginning of the tail. A 6-min test session was recorded. The behavioural parameter measured was the number of seconds spent in a completely immobile posture.

Forced swim test. The forced swim test was performed according to a modification, suggested by Lucki (Lucki, 1997), of the traditional method described by Porsolt (Porsolt et al., 1978). The following behavioural responses were recorded: escape or climbing behaviour, which was defined as upward-directed movement of the forepaws along the side of the swim chamber; swimming behaviour, which was defined as movement throughout the swim chamber; and immobility, which was recorded when the rat made no further attempts to escape except the movement necessary to keep its head above the water.

Tissue preparation and subcellular fractionation

Rats were sacrificed by rapid decapitation and the cortices and hippocampi were immediately separated on ice and placed in homogenization buffer (0.32 M sucrose, 0.5 mM EGTA, 5 mM Hepes, pH 7.4) supplemented with a mixture of protease inhibitors (Boehringer, Mannheim). Subcellular fractionation was performed following the method of Wyneken et al. (Wyneken et al., 2001). Synaptosomes were collected from the first sucrose gradient at the 1/1.2 M interphase and submitted to a hypo-osmotic shock to release intracellular organelles. Synaptic membranes were collected from the second sucrose gradient at the 1/1.2 M interphase and delipidated in 0.5% Triton to yield PSDs. The microsomal fraction (P3) resulted from the centrifugation of the supernatant (S2) at 100,000 g for 1 h. Protein concentrations were determined using the BCA assay (Pierce, Rockford, IL, USA).

Co-immunoprecipitations

Protein (250 μg) was solubilized for 2 h in 1 ml of solubilization buffer (50 mM Tris–Cl, 1% deoxycholate plus protease inhibitors, pH 9.0). The corresponding primary antibody or control IgG (2 μg) was added to the supernatant and incubated overnight. Protein G Sepharose (20 μl pre-washed with solubilization buffer and blocked with 0.2% BSA) was added and incubated for 1 h. The samples were centrifuged for 5 min at 1000 g and the supernatants were discarded. The immunoprecipitates were washed three times with solubilization buffer and were resuspended in 60 μl of electrophoresis loading buffer.

Immunostaining

Western blots. Equal amounts of protein (20 μg) were separated by 4–20% SDS gradient gel electrophoresis, transferred to nitrocellulose membranes and immunoblotted with the indicated primary and corresponding secondary antibodies.

Synaptic membranes. Synaptic membranes were immunostained following the procedure of Ciruela (Ciruela et al., 2006). Synaptic membranes were plated on polylysine-coated slides, fixed in 4% paraformaldehyde in PBS containing 4% sucrose for 10 min and washed with PBS containing 25 mM glycine. Membranes were permeabilized, blocked and incubated with the indicated primary antibody. After incubation with the primary antibody, the membranes were washed and stained with the corresponding secondary antibody (1:600; Alexa Fluor® 647 conjugated goat anti-Guinea-pig IgG, Alexa Fluor® 488 conjugated goat anti-rabbit IgG or Alexa Fluor® 555 conjugated donkey anti-mouse IgG; Invitrogen, Eugene, OR, USA). Images of serial sections were captured with a Nikon Eclipse TE2000-U inverted epifluorescence microscope with a Plan Fluor 60×/1.25 numeric aperture oil-immersion objective attached to a cooled monochrome camera DS-2MBWc (final magnification 3500×).

Immunohistochemistry. After perfusion, brains were cryopreserved and cut serially in 30-μm frozen coronal sections. Staining was performed according to Ampuero and collaborators (Ampuero et al., 2007). Immunoreactivity for the RSGb was quantified in coronal sections restricted to interaural 5.86 mm/bregma −3.14 mm and interaural 4.84 mm/ bregma −4.16 mm. Quantification of immunoreactivity in the PrL and M2 regions was restricted to interaural 13.20 mm/bregma 4.20 mm and interaural 11.20/bregma 2.20 mm (Paxinos and Watson, 1998). Layer V pyramidal neurons were examined in the RSGb and PrL area. In M2, layer II/III pyramidal neurons were analysed. Brain slices were visualized under a light microscope (AxiosKop, Zeiss, Germany; 10× magnification; numeric aperture 0.3), and images of serial sections were captured with a digital camera (Nikon, CoolPIX 995) with a final magnification of 880×. Digitized images were analysed with ImageJ program. The number of positive cells was counted in equal sample areas of 0.0289 mm^2. At least five sections per animal were analysed in control and treated animals (n=5 per group).

Spine analysis

Brains were processed using the FDRapid GolgiStainTM kit (FD Neuro Technologies, Baltimore, USA) (Ampuero et al., 2007) and analysed by an individual blind to the experimental conditions. Eighteen to twenty-three randomly selected layer V pyramidal neurons were examined per experimental condition in the RSGb and PrL area. In M2, layer II/III pyramidal neurons were analysed. The selected neurons were required to have no breaks in staining along the dendrites. Starting from the origin of the soma (for primary dendrites) or the branch point (for secondary dendrites) and continuing away from the cell soma, spines were counted in 8 μm segments along an 80 μm stretch of the dendrite. Dendritic spines were classified under the microscope at different focal planes, by a single rater, blinded to the experimental groups, into three shape categories (Harris et al., 1992): filopodia/thin, stubby and mushroom/branched spines. Thin spines had a greater length than neck diameter and similar head and neck diameters. Stubby spines had neck diameters that were similar to the total spine length. For mushroom-shaped spines, the diameter of the head was much greater than the diameter of the neck. Branched spines had more than one head emerging from a single neck originating from the dendrite. If there was ever any doubt in a classification (less than 10%), spine and neck diameters were measured from the picture taken at the focal plane in which it appeared at its maximal size.

Over 1200 spines from 18 to 23 neurons (four to five neurons per animal) were analysed per condition. In addition, images from each analysed dendritic segment were captured as visual support at 1 μm-spaced focal plane in the region of interest using a BX61 Olympus microscope (100× objective, numeric aperture 1.3) attached to a Diagnostic Instruments 25.4/2 MP camera (final magnification of 4700×; see movie in supplementary material).

Statistical analysis

Data were analysed using Graph Pad Prism 4.0 software and presented as mean±SEM. The statistical test used for behavioural data was one-way analysis of variance (ANOVA) followed by Newman–Keuls post hoc test for multiple comparisons. For morphological and immunochemical staining, the Mann–Whitney U-test was applied. In WBs, the relative optic densities of bands were compared by two-tailed t-tests. A probability level of $P<0.05$ (*) or $P<0.01$ (**) was accepted as significant.

RESULTS

Twenty-eight days of 0.7 mg/kg fluoxetine reduced anxiety and learned helplessness in rats

To evaluate meaningful changes elicited by flx, we first examined behaviour using two different flx doses, 0.7 mg/kg (0.7 flx) or 3.5 mg/kg (3.5 flx), to select a dose with optimal effects following 4 weeks of treatment. Although selective serotonin reuptake inhibitors are known to induce anorectic effects in rats, there was no significant difference in body weight gain among the experimental groups examined in this study (sal group, 140.8±6.2%; 0.7 flx group, 126±4%; 3.5 flx group, 131.4±4.1%; compared to day 1 of treatment). This may be due to the low doses of flx used in the present study. Interestingly, treatment with 0.7 mg/kg flx has already been shown to lead to plasma levels considered therapeutically effective in humans, and this dose stimulates BDNF/TrkB signalling at excitatory synapses (Wyneken et al., 2006).

We first assessed anxiety-like behaviour in the NSF test (Fig. 1A, left panel). The NSF test is a behavioural paradigm that is sensitive to chronic antidepressant treatments and acute treatments with anxiolytics (such as benzodiazepines) but not subchronic antidepressant treatments. In the NSF test, the latency to feed decreased from 396.9±39.8 s to 257.3±34.2 s in the 0.7 flx group and to 272.3±37.6 s in the 3.5 flx group ($F_{(2,16)}$=3.819; both groups $P<0.05$ compared to sal). After the test session, animals were returned to the home cage and allowed to eat. Next, we measured spontaneous motor activity because a change in this activity might indirectly influence behavioural tests. Although the flx-treated rats revealed a trend towards decreased motor activity, this was not significant when counted over a 30 min period (sal group, 1482±119.7, 0.7 flx group, 1388±113.3, 3.5 flx group, 1303±140.3; ($F_{(2,29)}$=0.4963)). Because rearings are positively correlated with anxiety (Velisek, 2006), we also examined the number of rearings as an index of vertical exploratory behaviour. We found significantly increased rearing in the 3.5 flx group compared to the 0.7 flx group ($P<0.05$) (sal group, 30±2.2, 0.7 flx group, 21.1±2.2, 3.5 flx group, 37.6±7.3; $F_{(2,29)}$=3.872; $P<0.05$). Although a trend towards decreased rearing with 0.7 flx treatment was

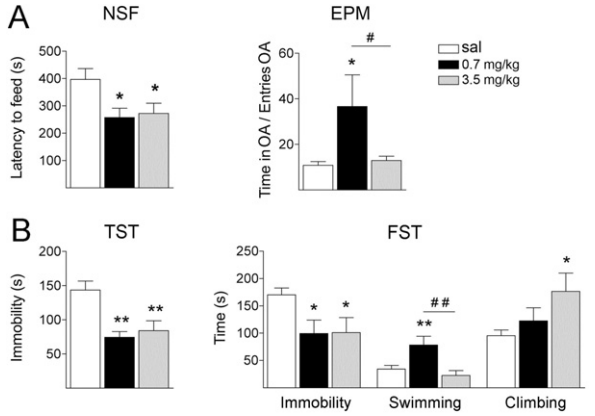

Fig. 1. Fluoxetine decreases depressive-like behaviours in rats. Rats were treated for 28 days with sal (white bars), 0.7 (black bars) or 3.5 (grey bars) mg/kg of flx. (A) Anxiety was analysed using the NSF test and the EPM test. Performances were video-recorded and analysed blindly. In the EPM, the time spent in the open arms divided by the number of entries into the open arms is shown. (B) Learned helplessness was assessed by the TST and the FST. In both cases, immobility was scored (in seconds). In addition, swimming and climbing behaviours were measured separately in the FST. Results are presented as mean±SEM. * $P<0.05$; ** $P<0.01$: compared to sal; # $P<0.05$: 3.5 flx compared to 0.7 flx; ## $P<0.01$: 3.5 flx compared to 0.7 flx (one-way ANOVA followed by post hoc test).

evident, the difference between the sal and 0.7 or 3.5 flx groups did not reach significance. Anxiety-like behaviour was also evaluated in the EPM test, which has been widely validated to measure anxiety in rodents (Pellow et al., 1985; Holmes et al., 2003). In the EPM test (Fig. 1A, right panel), the time in the open arm per entry increased in the rats treated with 0.7 flx ($F_{(2,23)}=5.227$; $P<0.05$). The Newman–Keuls post hoc multiple comparisons revealed that the scores of the 3.5 flx group were not different from controls. In addition, the 0.7 flx group scores differed from those of both the sal and the 3.5 flx groups ($P<0.05$). These results confirm that the 0.7 mg/kg dose is more efficient in decreasing anxiety.

Learned helplessness was assessed by the TST and the FST (Fig. 1B). In both tests, immobility decreased following 0.7 or 3.5 flx treatment. In the TST ($F_{(2,23)}=8.937$, $P<0.01$), the post hoc Newman-Keuls test revealed a significant decrease for both flx doses compared with sal ($P<0.01$). In the FST ($F_{(2,23)}=4.655$, $P<0.05$), the post hoc test revealed a significant decrease for both 0.7 and 3.5 flx ($P<0.01$ and $P<0.05$, respectively). However, only the 0.7 flx dose caused a significant increase in swimming behaviour when compared to the sal and 3.5 flx doses ($F_{(2,24)}=7.036$ $P<0.01$). The post hoc test revealed a significant effect ($P<0.01$) for 0.7 flx compared to sal and 3.5 flx. In this same test, the climbing behaviour was increased by 3.5 flx but not by 0.7 flx ($F_{(2,23)}=3.934$, $P<0.05$, and $P<0.05$ in the Newman-Keuls test comparing sal with 3.5 flx). Although both flx doses decreased immobility, the lower dose enhanced swimming behaviour, and the higher dose increased climbing behaviour. Overall, these results established that 0.7 flx for 28 days consistently induced antidepressant-like behavioural effects (reducing both anxiety and learned helplessness). Therefore, the 0.7 mg/kg dose of flx was chosen for subsequent analyses of structural and molecular effects at glutamatergic forebrain synapses.

Long-term flx induces subunit-specific changes in glutamate receptor subunit levels

Initially, we measured the levels of glutamate receptor subunits in forebrain homogenates by WB (Fig. 2A). We detected a large increase in GluR1 ($P<0.01$), GluR2 ($P<0.05$), NR2A and NR1 ($P<0.01$%), in the homogenates, but no change was found for NR2B. PSD-95 and SAP102 are examples of glutamate receptor scaffolding proteins, which have been implicated in the trafficking and anchoring of glutamate receptor subunits. In the present study, we did not detect any changes in PSD-95, but SAP102 increased by 60±6%. To check these results in cerebrocortical subregions, we performed IHC in coronal sections of the forebrain. In Fig. 2B (upper panel), two of the selected regions are shown: the PrL cortex, a subregion of the prefrontal cortex thought to modulate depressive symptoms (Sairanen et al., 2007; Muigg et al., 2008) and the RSGb, a limbic cortex on the posterior cingulate gyrus that has recently been implicated in the control of emotions (Maddock, 1999; Kumar et al., 2008). Fig. 2B (lower panel) shows representative stainings of NR2A and GluR2 at two different magnifications. The quantification of layer V-immunopositive cells revealed an increase of NR2A, NR2B, GluR1 and GluR2 in the RSGb area, whereas no change was found in the PrL area (Fig. 2C).

To determine whether the upregulated receptors were transported to the synapse, glutamate receptor subunits were detected by WB in isolated PSDs (Fig. 3A). We found no change in NR2B even though NR1 and NR2A subunits increased. In addition, the AMPA-R subunit GluR2 did not change, but GluR1 was decreased by 12±5% and the glutamate receptor scaffolding proteins PSD-95 and SAP102 were increased by 23±7% and 30±4%, respectively (not shown). Thus, treatment with flx appeared to favour synapses with higher ratios of NR2A to NR2B and GluR2 to GluR1. A possible explanation of decreased AMPA-R detection in PSDs is that GluR1 and GluR2 subunits, although increased in homogenates, might be preferentially localized intracellularly. To test this hypothesis, we used WB to determine that glutamate receptor subunits in the microsomal P3 fraction (Fig. 3B). This fraction is a heterogeneous membrane compartment known to be enriched in endoplasmic reticulum, Golgi network, endosomes, trafficking vesicles and synaptic vesicles, but not in PSDs (see Suppl. Fig. 1). Consistent with our previous data, we found increases of NR2A ($P<0.05$) whereas NR2B decreased ($P<0.01$). NR1 content was not modified. Significantly elevated GluR1 and GluR2 were found ($P<0.05$ in both cases) suggesting that these subunits are present in intracellular membranes, which contain a variety of cellular components including trafficking compartments. Another possibility was that AMPA-Rs were lost during the PSD purification procedure because they are loosely attached to PSDs and a proportion of them is localized on their periphery. Therefore, we used immunodetection to determine AMPA-R subunit localization in synaptic membranes, which are the cellular fractions from which PSDs

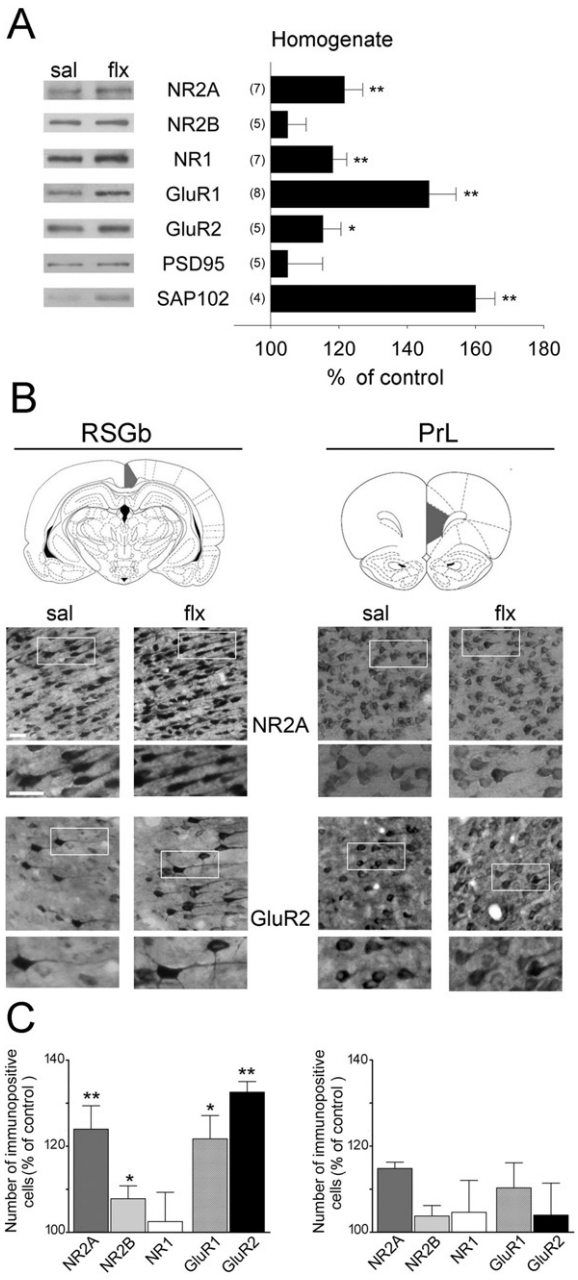

Fig. 2. Fluoxetine induces region-specific changes in glutamate receptor levels. (A) WBs of glutamate receptor subunits (NR2A, NR2B, NR1, GluR1 and GluR2) and scaffolding proteins (PSD-95 and SAP102) in cortical homogenates are shown. The left panel shows representative western blots for each protein, and the right panel shows the mean change of control ± SEM obtained by densitometric quantification of WBs. The number of independent experiments is indicated. (B) Glutamate receptor subunits were immunodetected in coronal sections through the rat cortex in the indicated brain areas (after Paxinos and Watson, 2008) (RSGb: retrosplenial granular cortex b; PrL: prelimbic cortex). Below, representative photomicrographs of NR2A and GluR2-stained sections are shown (scale bar: 25 μm). (C) Quantification of immunopositive cells expressed as change over control. Significant increases were found in the number of NR2A, NR2B, GluR1 and GluR2 positive cells in the RSGb but not in the PrL. Results are presented as mean±SEM and were determined from analysing 4–6 sections of five rats per group. Data were statistically evaluated with Mann–Whitney *U*-test, * $P<0.05$; ** $P<0.01$.

are obtained by delipidation. Synaptic membranes corresponded to synaptosomes that had been subjected to an osmotic shock to release intracellular membranes (i.e., their microsomal compartment). For increased sensitivity in this analysis compared to WBs, we stained synaptic membranes fixed on slides and quantified the levels of receptor subunits present exclusively in membrane compartments containing the scaffolding protein ProSAP2/Shank3, a reliable marker of excitatory synapses (Fig. 3C). As a positive control, we quantified the co-localization of NR2A and ProSAP2. Consistent with the WBs and immunohistochemical analysis, we found a significant increase of NR2A localization at excitatory synapses after flx treatment (Fig. 3D, left panel, $P<0.01$). Interestingly, the size of the stained membranous structures, corresponding to spines that frequently retain their presynaptic terminal, was augmented (Fig. 3D, right panel, $P<0.05$). This observation was consistent with the idea that NR2A subunits are present on larger spines. A similar analysis for GluR1 and GluR2 reflected no change in GluR1/ProSAP2 co-localization but a significant increase in GluR2/ProSAP2 colocalization ($P<0.05$). In both cases, the synaptic membrane area increased ($P<0.05$). These results suggested that AMPA-Rs present in the spine membrane preferentially contain GluR2 subunits and confirm that NMDA-Rs preferentially contain NR2A over NR2B. To test whether the subunit composition of N-methyl-D-aspartate (NMDA) and AMPA-Rs changed following flx, we co-immunoprecipitated relevant subunits from PSDs, synaptic membranes and synaptosomes as starting material. Fig. 3E shows representative immunoprecipitations of NR1 and GluR2 subunits from PSDs. Following flx, NR2A increased by 4.50±0.88 times over control in NR1 immunoprecipitates ($n=3$, $P<0.05$) and no change was observed for NR2B. GluR1 decreased in GluR2 immunoprecipitates to 0.62±0.11 when compared to sal ($n=4$, $P<0.05$). This was confirmed by immunoprecipitations from synaptic membranes in which the decrease of GluR1 was found to be 0.59±0.13 ($n=3$, $P<0.05$). However, when synaptosomes (i.e. synaptic membranes containing intracellular membranes) were taken as starting material for immunoprecipitation ($n=4$), no significant differences in AMPA-R stoichiometry were found (1.07±0.14). These results indicate that at the level of the spine membrane, flx induced a switch towards AMPA-Rs preferentially enriched in GluR2 subunits and of NMDAR-Rs enriched in NR2A subunits. In contrast, GluR1 was increased but it might accumulate in intracellular locations. Taken together, these results confirm that GluR1 might not reach dendritic spine membranes or PSDs even though immunohistochemistry and WBs demonstrated that it was increased.

Changes in dendritic spine density and morphology after 28 days of flx

To determine whether changes in glutamate receptor subunit composition were associated with changes in spine morphology, we performed Golgi stainings in the described cortical subregions (Fig. 4 and movie in Supplementary Material). Fig. 4A shows representative inverted images,

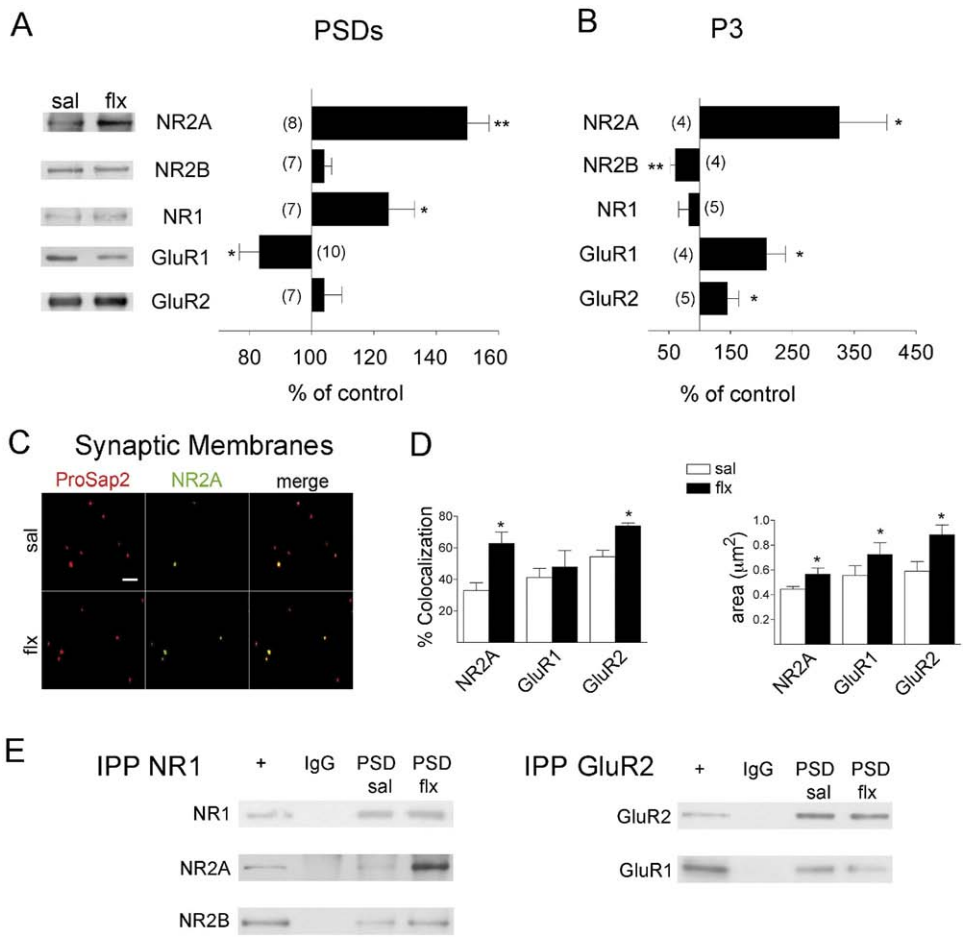

Fig. 3. Fluoxetine-induced changes on AMPA and NMDA-R subunit levels. (A) Western blots of glutamate receptor subunits in isolated postsynaptic densities (PSDs) are shown. Left panel shows representative western blots for each protein, and the right panel shows the mean change of control ± SEM obtained by densitometric quantification of western blots. Note that GluR1 decreases in PSDs. The number of independent determinations is indicated. (B) Quantification of glutamate receptor subunits detected by western blots in the microsomal fraction (P3), which is enriched in intracellular membranes but not PSDs. (C) Immunocytochemical identification of NR2A (green) in the glutamatergic population of synaptic membranes (identified as ProSAP2/Shank3 immunoreactive; red). In the superimposed picture of the double immunocytochemical labelling (merge) of these representative fields, co-localization was quantified (scale bar: 5 μm). (D) The left panel shows the quantification of co-localization of five different fields per slide from four independent experiments using different membrane preparations and confirmed the augmented co-localization of NR2A and GluR2 but not of GluR1 with isolated glutamatergic synapse compartments. In the right panel, the size of the double-positive membrane compartments was calculated. Note that the synaptic membranes correspond to synaptosomes that were subjected to a hypo-osmotic shock in order to release intracellular membranes. Results are presented as mean±SEM. Data were statistically evaluated with a paired *t*-test, * $P<0.05$; ** $P<0.01$. (E) Equal amounts of NR1 and GluR2 were immunoprecipitated from PSDs to evaluate changes in receptor stoichiometry. WBs of the corresponding subunits are shown. In NR1 immunoprecipitates, a large increase in NR2A (4.5±0.88; $P<0.05$) was found whereas a decrease of GluR1 (0.62±0.11; $P<0.05$) was found in GluR2-containing AMPA-Rs ($n=3$).

taken at three different focal planes, of a primary dendrite present in the RSGb of sal and flx treated animals and indicates the main morphological types (filopodia/thin, stubby and mushroom). Spine density was measured from its emergence from the soma along an 80 μm stretch of the primary apical dendrite that was subdivided into 10 segments (Fig. 4B). The number of spines per 8 μm segment increased beginning at the fifth segment in the RSGb and at the seventh segment in the PrL. This was accompanied by a robust increase in the percentage of mushroom-type spines and a decrease of thin spines in the RSGb (Fig. 4B, right panel, $P<0.01$). In the PrL, thin spines also decreased and stubby spines increased ($P<0.05$), but there was no change in mushroom-type spines. Therefore, the change in spine morphology was especially significant in the RSGb, which was the same region that revealed significant increases in glutamate receptor subunits excluding NR2B. To evaluate whether this is a more general phenomenon, secondary dendrites in these areas were examined (not shown), and the analysis was extended to the secondary motor cortex (M2, supplementary material), which is not thought to be directly involved in the modulation of depressive behaviours. For secondary dendrites, shorter segments (from 32 to 80 μm) were measured with the premise that the selected segment had to be continuous with the primary dendrite and the cell soma. In the case of the RSGb, total spine density (measured as the number of spines per μm) increased from 0.70±0.04 to 0.84±0.04 ($P<0.05$). Mushroom-type spines increased from 32.9% to 43.7% ($P<0.05$) with a concomitant de-

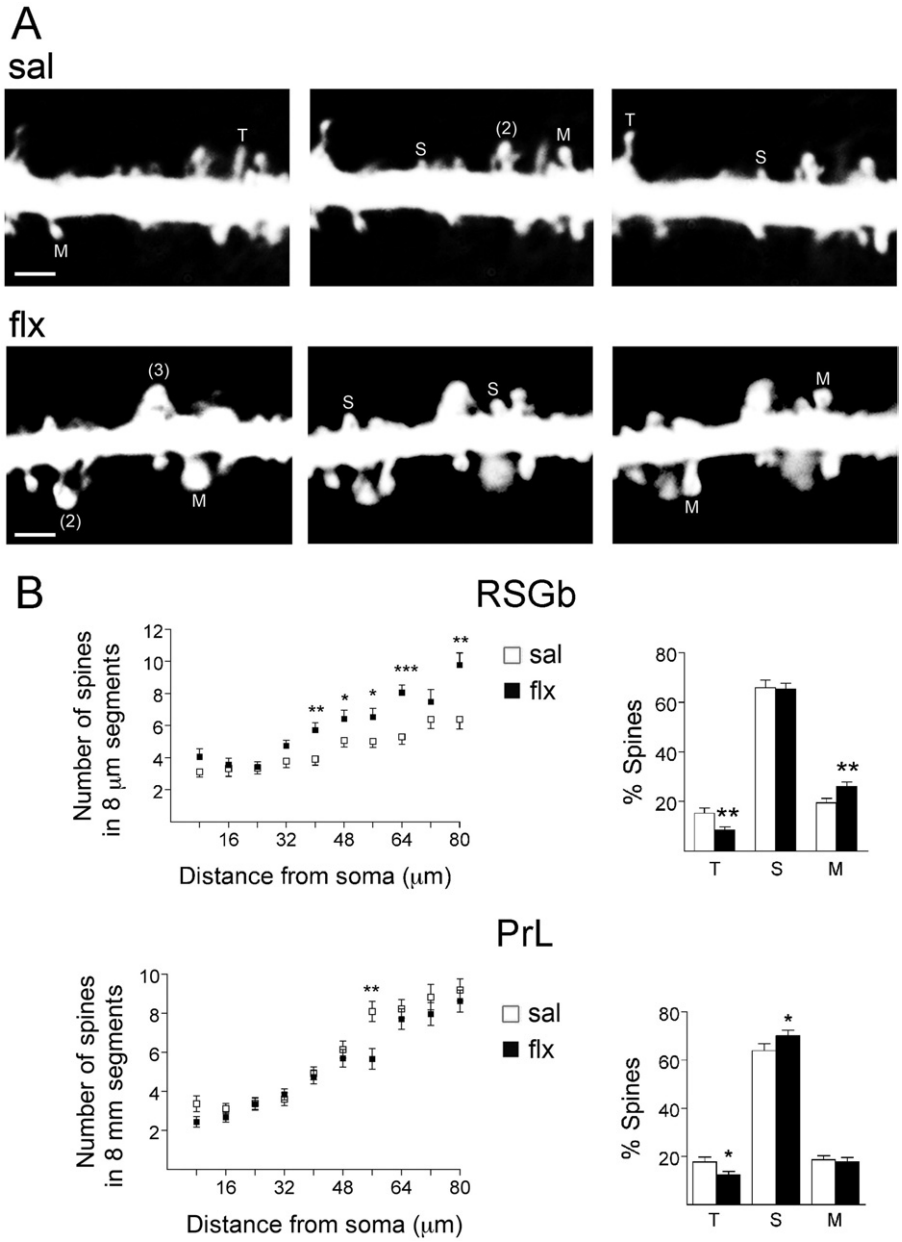

Fig. 4. The effect of flx on spine density and morphology. Cortical pyramidal neurons were visualized by the rapid Golgi impregnation method. (A) Representative images taken at three different focal planes in sal and flx-treated rats were inverted for better visualization. The original image, used for quantification at 12 different focal planes per dendritic segment, is presented in the supplementary material. The three shape categories of spines were shown as follows: filopodia/thin (T), stubby (S) and mushroom/branched (M). The numbers in parentheses indicate superimposed spines that were resolved by observation at different focal planes: (2) represents a thin and a mushroom-type spine in both cases and (3) represents a thin, a stubby and a mushroom-type spine. See experimental procedures and the movie in supplementary material for details. The scale bar was 1 μm. (B) The left panels show spine number along primary dendrites in consecutive dendritic segments of 8 μm away from the soma in the RSGb and the PrL. The right panels show the classification of dendritic spines, which revealed a significant increase of mushroom-type spines in the RSGb, but no differences in the PrL, between sal and flx treated animals. All results are presented as mean±SEM determined from analysing 18–23 cells/area obtained from five rats per group, * $P<0.05$; ** $P<0.01$.

crease of thin and stubby-like spines ($P<0.05$). In the PrL, no change in secondary spine density was found, and this was associated with no change in spine morphology. Interestingly, the changes in both spine morphology and glutamate receptor subunit levels extended to layer II/III of M2 (Suppl. Fig. 2).

Taken together, the results indicated that flx induced morphological and molecular changes affecting large forebrain areas. Increased mushroom-type spines in selected regions were accompanied by global increases of NR2A-containing NMDA-Rs and of GluR2-containing AMPA-Rs. GluR1 subunits, although upregulated, might be retained

in the cell soma, or they might be located near, or even within, spines. Surprisingly, such changes were highly significant in the RSGb but less prominent in the PrL cortex.

DISCUSSION

Our results were the first to demonstrate that long-term behaviourally relevant doses of flx induced an enrichment of specific glutamate receptor subunits in the rat forebrain. Whereas GluR2 and NR2A increased in spine membranes and PSDs, GluR1, although increased in homogenates and in immunohistochemical analysis, did not reach these synaptic compartments. Changes in subunits levels were associated with an increase of mushroom-type dendritic spines in a region-specific manner and were especially significant in the RSGb. The molecular changes observed here may underlie the restoration of plasticity previously observed in the visual cortex following flx (Maya Vetencourt et al., 2008). These changes are compatible with a "maturation-like" process leading to stabilization of synaptic connections that may be related to a functional recovery of glutamatergic forebrain networks (Castren, 2005; Wyneken et al., 2006).

Our behavioural data showed that the flx dose used in the long-term studies is an important variable to be considered. Consistent with our results, a similar low-dose of flx (1 mg/kg) induced antidepressant-like effects and effectively modulated neuronal firing rates (Contreras et al., 2001; Rodriguez-Landa et al., 2003). Conflicting data regarding mechanisms involved in antidepressant action might be due to the use of potentially harmful doses (Wyneken et al., 2006). Increased fear has been reported following 10 mg/kg flx treatment in the EPM (Schulz et al., 2007). Our results indicated that 3.5 mg/kg flx was not effective in reducing anxiety-like behaviour in the EPM or rearing but was effective in the NSF. Although both the NSF and EPM are conflict tests to assess anxiety, they recruit different neuronal circuits. NSF depends crucially on appetite drive whereas the EPM depends on exploratory behaviour (Sousa et al., 2006). Consistent with our findings, contrasting results using both tests have previously been reported, and it has been proposed that the EPM may show a decreased sensitivity to chronic antidepressant treatment as well as high drug doses (Lira et al., 2003). A differential dose-dependent effect was confirmed in the FST. Climbing, a behaviour considered to be dependent on noradrenergic neurotransmission, was favoured over swimming after 3.5 flx but not 0.7 flx (Cryan et al., 2002, 2004; Vizi et al., 2004). In addition, both flx doses caused opposing trends on rearing behaviour that were not significant when compared to sal: treatment with 0.7 flx induced a decrease in the amount of rearing, and 3.5 flx treatment induced an increase resulting in a significant difference between the 0.7 and 3.5 flx doses ($P<0.05$). Increased rearing has been shown to correlate positively with anxiety-like behaviour (Borta and Schwarting, 2005; Velisek, 2006). Our results suggested that the 3.5 dose, in addition to modulating noradrenergic neurotransmission, might negatively affect anxiety-like behaviour (such as rearing) or have no effect (for instance, on EPM performance). In the future, behavioural studies of flx dosing should be undertaken in animals in which depressive-like behaviour is induced (e.g., by exposure to chronic stress).

Glutamate receptors and antidepressants

A strong relationship between mood disorders and glutamate neurotransmission has already been postulated (Kessels and Malinow, 2009), including antidepressant-like activity of NMDA-R antagonists and participation of AMPA-Rs, especially its GluR2 subunit (Gray et al., 2003; Gould et al., 2008). In agreement with our results, imipramine upregulated synaptic GluR2 (Du et al., 2008) and increased GluR1 in synaptosomes (Du et al., 2004). Increased GluR1 levels were found in a hippocampal synaptic fraction obtained from ovariectomized, but not control, rats treated with 5 mg/kg flx for 21 days (O'Leary et al., 2009). The difference in our results may be due to the flx dose or the time course of the molecular adaptations. Flx might counteract the decrease of NR2A, but not NR2B, observed in major depression (Beneyto and Meador-Woodruff, 2008) or the decreases of NR1, NR2A and SAP102 observed in bipolar disorder (McCullumsmith et al., 2007; Beneyto and Meador-Woodruff, 2008). Although both NMDA and AMPA-Rs may be particularly important targets for the treatment of mood disorders, we postulated that subunit-specific strategies should be considered.

Role of glutamate receptor subunits in structural and functional plasticity

The importance of NMDA-Rs in synaptic plasticity and memory are well described (Malenka and Bear, 2004). However, the potential opposing contributions of NR2A and NR2B subunits to LTP versus LTD have been highly controversial (Yashiro and Philpot, 2008). LTP itself might induce an immediate switch favouring NR2A over NR2B-containing receptors (Grosshans et al., 2002; Bellone and Nicoll, 2007). The switch of NR2B to NR2A containing NMDA-Rs during development is accompanied by synaptic maturation, stabilization and growth (Monyer et al., 1994). In contrast to NR2B subunits, NR2A subunits are predominantly present on large spines (Kobayashi et al., 2007; Shinohara et al., 2008). In accordance with this, the synaptic enrichment of NR2A induced by flx was accompanied by a higher proportion of mushroom-type spines, suggesting that flx might induce a maturation-like state.

NMDA-Rs regulate synaptic strength by controlling the trafficking of AMPA-Rs in and out of postsynaptic sites (Malenka and Bear, 2004). Synaptic strengthening involves activity-dependent addition of GluR subunits containing a long intracellular C-terminal tail (e.g. GluR1-containing) to synapses, whereas short-tailed subunits (GluR2 and GluR3) constitutively replace existing receptors. Therefore, inserted GluR1 subunits are later replaced by GluR2, although the requirement of this transient process is currently debated (Adesnik and Nicoll, 2007). A temporal characterization of synaptic changes induced by flx would be necessary to determine whether the switch towards GluR2-containing receptors required a preceding GluR1 insertion. The fact that we did not find changes in GluR1 or

NR1 content in PSDs 2 weeks after flx treatment indicates that these adaptations, measured after 4 weeks, are slowly induced (Wyneken et al., 2006).

A highly positive correlation also exists between GluR2 levels and synaptic size, spine density and mEPSC frequency, a relationship that has not been established for GluR1 (Passafaro et al., 2003; Saglietti et al., 2007; Antal et al., 2008). In addition, GluR2 is more stably tethered to the synapse and its incorporation is necessary for the long-term expression of synaptic plasticity (Isaac et al., 2007; Yao et al., 2008). The increased levels of the scaffolding proteins PSD-95 and SAP102 in homogenates and PSDs are consistent with their role in anchoring glutamate receptors and delivering critical elements to growing spines.

It is likely that the flx-induced effects on spine morphology and glutamate receptor content were mediated by neurotrophic factors (Tanaka et al., 2008). Several growth factors, including BDNF and vascular endothelial growth factor (VEGF) and their signalling pathways are necessary for a response to antidepressant drug treatment (Castren et al., 2007; Warner-Schmidt and Duman, 2008). Their specific contribution to the observed changes needs to be addressed in the future.

Morphological changes in the forebrain

Animal models currently used to elicit depressive-like symptoms lead to structural changes in neuronal networks, including dendritic length and complexity and spine morphology (Liston et al., 2006; Radley et al., 2006; McEwen, 2007). These changes can be reversed by antidepressant treatment (Hajszan et al., 2010; Bessa et al., 2009) suggesting that the flx-induced spine remodelling that we observed is involved in antidepressant action. Increases in spine density and mushroom-type spines in the RSGb and M2 might reflect enhanced basal neurotransmission. We observed region-specific changes that correlated with changes in glutamate receptor subunits. However, these effects probably extend to wide forebrain areas because changes in glutamate receptor subunits could be detected in subcellular fractions obtained from whole forebrain homogenates. Consistent with this idea, flx induced structural plasticity in the rat somatosensory cortex (Guirado et al., 2009). Cognitive-emotional behaviours rely on complex interactions of networks in several brain areas (Pessoa, 2008). The contribution of specific areas to depressive-like behaviours and antidepressant treatment is not completely understood. Besides mood disturbance, depression is accompanied by sensorimotor disturbances, and manipulating the motor system (e.g., by physical exercise) improves mood (Canbeyli, 2010). It is therefore conceivable that the structural modulation of M2 has some therapeutic significance. In turn, the RSGb is connected with cortices known to be involved in emotional control, such as the hippocampal formation and the midline limbic cortices (Van Groen and Wyss, 2003). Activation of the RSGb by emotionally salient stimuli has already been shown (Maddock, 1999). Interestingly, the retrosplenial cortex has been implicated in an experimental model of schizophrenia induced by NMDA receptor antagonists. Unexpectedly, in these studies it was found that the antagonists acted in an excitatory manner because the blocked NMDA-Rs were localized on GABAergic interneurons (Olney et al., 1991; Olney and Farber, 1995; Vaisanen et al., 1999; Morimoto et al., 2002; Dickerson and Sharp, 2006). It is possible that the therapeutic effect of NMDA receptor antagonists, at the subanaesthetic doses currently under investigation for the treatment of depression, is in part due to their pro-excitatory effect in the retrosplenial cortex (Krishnan and Nestler, 2008; Pittenger and Duman, 2008). In line with these results, the gray matter in bipolar disorder was reduced in the posterior cingulate/retrosplenial cortex of unmedicated subjects relative to medicated patients (Nugent et al., 2006). The interesting possibility that the plastic changes induced by flx in this cerebrocortical region might be related with its positive effects on emotion and cognition should be investigated in the near future. In general, these findings underscore the importance of discriminating between cortical subregions affected by antidepressants.

Several questions should be addressed in the future. For example, what are the cellular mechanisms that induce a *coordinated* switch of both NMDA and AMPA-R subunits? Are plastic changes in the glutamatergic system causally related to mood recovery? Can we identify brain circuits that are specifically related to a subset of depressive behaviours, and are the RSGb and M2 part of such circuits? In the future, relevant brain circuitries might be preferentially targeted by antidepressant treatments (e.g., by transcranial magnetic stimulation) in a personalized manner depending on individual symptomatology (Holsboer, 2008). Our findings might contribute to the search of new and faster-acting antidepressant interventions that target specific glutamate receptor subunits in concert as well as forebrain circuits critically involved in depressive symptoms.

The delayed molecular adaptations in extensive cortical networks reported here may underlie the therapeutic action of antidepressants. Our findings that a widely prescribed antidepressant in humans induces structural and molecular plasticity in the adult forebrain suggests a potential clinical application for antidepressants in neurological disorders in which synaptic function is compromised.

Acknowledgments—This work was supported by Proyecto Anillo ACT09-06 (U Wyneken). We are grateful to Soledad Sandoval for technical support.

REFERENCES

Adesnik H, Nicoll RA (2007) Conservation of glutamate receptor 2-containing AMPA receptors during long-term potentiation. J Neurosci 27:4598–4602.

Al-Hallaq RA, Conrads TP, Veenstra TD, Wenthold RJ (2007) NMDA di-heteromeric receptor populations and associated proteins in rat hippocampus. J Neurosci 27:8334–8343.

Alvarez VA, Ridenour DA, Sabatini BL (2007) Distinct structural and ionotropic roles of NMDA receptors in controlling spine and synapse stability. J Neurosci 27:7365–7376.

Ampuero E, Dagnino-Subiabre A, Sandoval R, Zepeda-Carreno R, Sandoval S, Viedma A, Aboitiz F, Orrego F, Wyneken U (2007) Status epilepticus induces region-specific changes in dendritic spines, dendritic length and TrkB protein content of rat brain cortex. Brain Res 1150:225–238.

Antal M, Fukazawa Y, Eordogh M, Muszil D, Molnar E, Itakura M, Takahashi M, Shigemoto R (2008) Numbers, densities, and colocalization of AMPA- and NMDA-type glutamate receptors at individual synapses in the superficial spinal dorsal horn of rats. J Neurosci 28:9692–9701.

Bellone C, Nicoll RA (2007) Rapid bidirectional switching of synaptic NMDA receptors. Neuron 55:779–785.

Beneyto M, Meador-Woodruff JH (2008) Lamina-specific abnormalities of NMDA receptor-associated postsynaptic protein transcripts in the prefrontal cortex in schizophrenia and bipolar disorder. Neuropsychopharmacology 33:2175–2186.

Bessa JM, Ferreira D, Melo I, Marques F, Cerqueira JJ, Palha JA, Almeida OF, Sousa N (2009) The mood-improving actions of antidepressants do not depend on neurogenesis but are associated with neuronal remodeling. Mol Psychiatry 14:764–773, 739.

Bleakman D, Alt A, Witkin JM (2007) AMPA receptors in the therapeutic management of depression. CNS Neurol Disord Drug Targets 6:117–126.

Borta A, Schwarting RK (2005) Inhibitory avoidance, pain reactivity, and plus-maze behavior in Wistar rats with high versus low rearing activity. Physiol Behav 84:387–396.

Canbeyli R (2010) Sensorimotor modulation of mood and depression: an integrative review. Behav Brain Res 207:249–264.

Castren E (2005) Is mood chemistry? Nat Rev Neurosci 6:241–246.

Castren E, Voikar V, Rantamaki T (2007) Role of neurotrophic factors in depression. Curr Opin Pharmacol 7:18–21.

Ciruela F, Casado V, Rodrigues RJ, Lujan R, Burgueno J, Canals M, Borycz J, Rebola N, Goldberg SR, Mallol J, Cortes A, Canela EI, Lopez-Gimenez JF, Milligan G, Lluis C, Cunha RA, Ferre S, Franco R (2006) Presynaptic control of striatal glutamatergic neurotransmission by adenosine A1-A2A receptor heteromers. J Neurosci 26:2080–2087.

Contreras CM, Rodriguez-Landa JF, Gutierrez-Garcia AG, Bernal-Morales B (2001) The lowest effective dose of fluoxetine in the forced swim test significantly affects the firing rate of lateral septal nucleus neurones in the rat. J Psychopharmacol 15:231–236.

Cryan JF, Markou A, Lucki I (2002) Assessing antidepressant activity in rodents: recent developments and future needs. Trends Pharmacol Sci 23:238–245.

Cryan JF, O'Leary OF, Jin SH, Friedland JC, Ouyang M, Hirsch BR, Page ME, Dalvi A, Thomas SA, Lucki I (2004) Norepinephrine-deficient mice lack responses to antidepressant drugs, including selective serotonin reuptake inhibitors. Proc Natl Acad Sci U S A 101:8186–8191.

Chen W, Prithviraj R, Mahnke AH, McGloin KE, Tan JW, Gooch AK, Inglis FM (2009) AMPA glutamate receptor subunits 1 and 2 regulate dendrite complexity and spine motility in neurons of the developing neocortex. Neuroscience 159:172–182.

Diaz-Veliz G, Mora S, Gomez P, Dossi MT, Montiel J, Arriagada C, Aboitiz F, Segura-Aguilar J (2004) Behavioral effects of manganese injected in the rat substantia nigra are potentiated by dicumarol, a DT-diaphorase inhibitor. Pharmacol Biochem Behav 77:245–251.

Dickerson J, Sharp FR (2006) Atypical antipsychotics and a Src kinase inhibitor (PP1) prevent cortical injury produced by the psychomimetic, noncompetitive NMDA receptor antagonist MK-801. Neuropsychopharmacology 31:1420–1430.

Du J, Creson TK, Wu LJ, Ren M, Gray NA, Falke C, Wei Y, Wang Y, Blumenthal R, Machado-Vieira R, Yuan P, Chen G, Zhuo M, Manji HK (2008) The role of hippocampal GluR1 and GluR2 receptors in manic-like behavior. J Neurosci 28:68–79.

Du J, Gray NA, Falke CA, Chen W, Yuan P, Szabo ST, Einat H, Manji HK (2004) Modulation of synaptic plasticity by antimanic agents: the role of AMPA glutamate receptor subunit 1 synaptic expression. J Neurosci 24:6578–6589.

Gould TD, O'Donnell KC, Dow ER, Du J, Chen G, Manji HK (2008) Involvement of AMPA receptors in the antidepressant-like effects of lithium in the mouse tail suspension test and forced swim test. Neuropharmacology 54:577–587.

Gray NA, Du J, Falke CS, Yuan P, Manji HK (2003) Lithium regulates total and synaptic expression of the AMPA glutamate receptor GluR2 in vitro and in vivo. Ann N Y Acad Sci 1003:402–404.

Grosshans DR, Clayton DA, Coultrap SJ, Browning MD (2002) LTP leads to rapid surface expression of NMDA but not AMPA receptors in adult rat CA1. Nat Neurosci 5:27–33.

Guirado R, Varea E, Castillo-Gomez E, Gomez-Climent MA, Rovira-Esteban L, Blasco-Ibanez JM, Crespo C, Martinez-Guijarro FJ, Nacher J (2009) Effects of chronic fluoxetine treatment on the rat somatosensory cortex: activation and induction of neuronal structural plasticity. Neurosci Lett 457:12–15.

Hajszan T, Szigeti-Buck K, Sallam NL, Bober J, Parducz A, Maclusky NJ, Leranth C, Duman RS (2010) Effects of estradiol on learned helplessness and associated remodeling of hippocampal spine synapses in female rats. Biol Psychiatry 67:168–174.

Harris KM, Jensen FE, Tsao B (1992) Three-dimensional structure of dendritic spines and synapses in rat hippocampus (CA1) at postnatal day 15 and adult ages: implications for the maturation of synaptic physiology and long-term potentiation. J Neurosci 12:2685–2705.

Holmes A, Kinney JW, Wrenn CC, Li Q, Yang RJ, Ma L, Vishwanath J, Saavedra MC, Innerfield CE, Jacoby AS, Shine J, Iismaa TP, Crawley JN (2003) Galanin GAL-R1 receptor null mutant mice display increased anxiety-like behavior specific to the elevated plus-maze. Neuropsychopharmacology 28:1031–1044.

Holsboer F (2008) How can we realize the promise of personalized antidepressant medicines? Nat Rev Neurosci 9:638–646.

Isaac JT, Ashby M, McBain CJ (2007) The role of the GluR2 subunit in AMPA receptor function and synaptic plasticity. Neuron 54:859–871.

Kessels HW, Malinow R (2009) Synaptic AMPA receptor plasticity and behavior. Neuron 61:340–350.

Kobayashi C, Aoki C, Kojima N, Yamazaki H, Shirao T (2007) Drebrin a content correlates with spine head size in the adult mouse cerebral cortex. J Comp Neurol 503:618–626.

Kopec C, Malinow R (2006) Neuroscience. Matters of size. Science 314:1554–1555.

Krishnan V, Nestler EJ (2008) The molecular neurobiology of depression. Nature 455:894–902.

Kumar P, Waiter G, Ahearn T, Milders M, Reid I, Steele JD (2008) Abnormal temporal difference reward-learning signals in major depression. Brain 131:2084–2093.

Lira A, Zhou M, Castanon N, Ansorge MS, Gordon JA, Francis JH, Bradley-Moore M, Lira J, Underwood MD, Arango V, Kung HF, Hofer MA, Hen R, Gingrich JA (2003) Altered depression-related behaviors and functional changes in the dorsal raphe nucleus of serotonin transporter-deficient mice. Biol Psychiatry 54:960–971.

Liston C, Miller MM, Goldwater DS, Radley JJ, Rocher AB, Hof PR, Morrison JH, McEwen BS (2006) Stress-induced alterations in prefrontal cortical dendritic morphology predict selective impairments in perceptual attentional set-shifting. J Neurosci 26:7870–7874.

Lucki I (1997) The forced swimming test as a model for core and component behavioral effects of antidepressant drugs. Behav Pharmacol 8:523–532.

Maddock RJ (1999) The retrosplenial cortex and emotion: new insights from functional neuroimaging of the human brain. Trends Neurosci 22:310–316.

Malenka RC, Bear MF (2004) LTP and LTD: an embarrassment of riches. Neuron 44:5–21.

Maya Vetencourt JF, Sale A, Viegi A, Baroncelli L, De Pasquale R, O'Leary OF, Castren E, Maffei L (2008) The antidepressant fluoxetine restores plasticity in the adult visual cortex. Science 320:385–388.

McClung CA, Nestler EJ (2008) Neuroplasticity mediated by altered gene expression. Neuropsychopharmacology 33:3–17.

McCullumsmith RE, Kristiansen LV, Beneyto M, Scarr E, Dean B, Meador-Woodruff JH (2007) Decreased NR1, NR2A, and SAP102 transcript expression in the hippocampus in bipolar disorder. Brain Res 1127:108–118.